Journal of Applied Polymer Science

Optical, Electrochemical, and Photovoltaic Properties of Conjugated Polymers with Dithiafulvalene as Side Chains

Chuantao Gu,[1,2] Zhengkun Du,[1,2] Wenfei Shen,[1,3] Xichang Bao,[1] Shuguang Wen,[1] Dangqiang Zhu,[1,2] Ting Wang,[1] Ning Wang,[1] Renqiang Yang[1]

[1]CAS Key Laboratory of Bio-based Materials, Qingdao Institute of Bioenergy and Bioprocess Technology, Chinese Academy of Sciences, Qingdao 266101, China

[2]University of Chinese Academy of Sciences, Beijing 100049, China

[3]Institute of Hybrid Materials, Laboratory of New Fiber Materials and Modern Textile—The Growing Base for State Key Laboratory, Qingdao University, Qingdao 266071, China

Correspondence to: R. Yang (E-mail: yangrq@qibebt.ac.cn)

ABSTRACT: Three conjugated polymers, P1–P3, with dithiafulvalene (DTF) as side chains have been synthesized. All polymers have good thermal stabilities. The DTF unit could be oxidized to $DTF^{\bullet+}$ which was observed from cyclic voltammetry and ultraviolet–visible (UV–vis) spectra, and the oxidation process was independent of the conjugated backbone of the polymer. The strong π–π^* transition absorbing band of the three polymers decreases gradually as increasing oxidation, and the resulting $DTF^{\bullet+}$ species give rise to an additional band at 750–1100 nm, which can be assigned to a distinguishing feature of the cation radical species. Photovoltaic device based on the blend of **P2** and [6,6]-phenyl-C61-butyric acid methyl ester ($PC_{61}BM$) showed the power conversion efficiency of 1.05% with a fill factor of 42.8%. © 2014 Wiley Periodicals, Inc. J. Appl. Polym. Sci. **2015**, *132*, 41508.

KEYWORDS: adsorption; applications; copolymers; electrochemistry

Received 24 June 2014; accepted 7 September 2014
DOI: 10.1002/app.41508

INTRODUCTION

Conjugated polymers, which are comprised of two or more π-conjugated repeat units and typically made by step-growth or condensation polymerization reactions, are promising for the application in organic electronics,[1–3] such as polymer solar cells (PSCs),[4–7] organic light-emitting diodes (OLEDs),[8] thin film transistors (TFTs),[9] and microelectronics.[10] The design and synthesis of new conjugated polymers have attracted great attention in the field of organic semiconductors because of their convenient preparation, low processing temperature, and nearly unlimited variability.[11] The benefits of versatile polymer syntheses allow for the effective tailoring of the intrinsic properties of conjugated polymers to serve the desired purpose and address the application needs.[12–14]

Tetrathiafulvalene (TTF) has been extensively used in modern materials science and organic electronics.[15–20] It is well-known that TTF and its derivatives can exist in three stable states (TTF^0, $TTF^{\bullet+}$ and TTF^{2+})[21,22] and have a strong propensity to self-assemble into regular π-stacks.[11] Dithiafulvalenes (DTFs), similar to TTFs, exhibit unique charge transport characteristics because of their coplanar molecular structures with strong π–π and S•••S interactions.[23] Thus, grafting DTF units on conjugated polymers may well utilize the strong self-assembling propensity of DTFs to increase the long-range order of the conjugated chains and improve the charge-carrier mobility of the polymers. Recently, two similar DTF-fused conjugated polymers were reported by Chen and coworkers.[23] The polymers exhibit strong π–π stacking interaction and good carrier mobility. Inspired by this work, Lin and coworkers reported three conjugated polymers based on DTF moiety for PSCs,[24] and the power conversion efficiency (PCE) reached 0.93%, which was significantly higher than those of TTF-based polymers.[11,20] To our best knowledge, this was the only report on the photovoltaic properties of DTF-based polymers, and there is no further investigation on the spectroelectrochemical properties of DTF-based polymers.

In this work, considering the strong self-assembling propensity of DTFs, this block was grafted on the polymers to increase the long-range order of the conjugated main chains. The structures are shown in Scheme 1. The electrochemical properties and optical responses to electrochemical redox processes were

Additional Supporting Information may be found in the online version of this article.

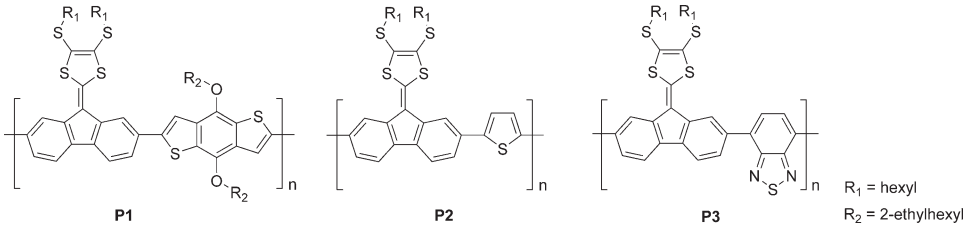

Scheme 1. Chemical structures of **P1–P3.**

carefully examined and the results showed that the DTF units could be oxidized to DTF•$^+$. PSCs based on the polymers have been fabricated and characterized. The device based on **P2**:[6,6]-phenyl-C61-butyric acid methyl ester ($PC_{61}BM$) (1 : 1, wt/wt) showed the best PCE of 1.05% with an open circuit voltage (V_{oc}) of 0.80 V, a short circuit current density (J_{sc}) of 3.07 mA cm^{-2}, and a fill factor (FF) of 42.8%, which was the highest one among the DTF- and TTF-based polymers.

EXPERIMENTAL

Materials

All reagents and starting materials were purchased from commercial sources and used without further purification unless otherwise noted. All air and water sensitive reactions were performed under nitrogen atmosphere. Toluene and tetrahydrofuran (THF) were distilled from sodium, with benzophenone as an indicator.

Characterization

^{1}H-NMR spectra were recorded on a Bruker Advance III 600 (600 MHz). Ultraviolet–visible (UV–vis) absorption spectra were recorded at room temperature using Hitachi U-4100 spectrophotometer. Cyclic voltammetry (CV) measurements were performed on a CHI 660D electrochemical workstation. It is equipped with a three-electrode cell consisting of a platinum disk working electrode (2.0 mm in diameter), a saturated calomel reference electrode (SCE), and a platinum wire counter electrode. The measurements were carried out in anhydrous acetonitrile containing 0.1*M* tetrabutylammonium phosphorus hexafluoride (Bu_4NPF_6) as supporting electrolyte under nitrogen atmosphere at a scan rate of 50 mV s^{-1}. Thin films were deposited from chloroform solution onto the platinum working electrodes and dried under nitrogen prior to measurement. The redox potential of the ferrocene/ferrocenium (Fc/Fc^+) internal reference is 0.39 V vs. SCE. The lowest unoccupied molecular orbital (LUMO) and highest occupied molecular orbital (HOMO) energy levels were determined by calculating the empirical formulas of $E_{HOMO} = -(E_{ox} + 4.80 - E_{1/2,(Fc/Fc+)})$, $E_{LUMO} = -(E_{red} + 4.80 - E_{1/2,(Fc/Fc+)})$, where E_{ox} and E_{red} were the onset oxidation and reduction potentials, respectively. Thermogravimetric analysis (TGA) measurements were performed by a STA-409 at a heating rate of 10°C min^{-1}, under the protection of nitrogen atmosphere. X-ray diffraction (XRD) spectra were recorded on a Bruker D8 Advance. Gel permeation chromatography (GPC) analyses were made using THF as eluant. FTIR spectra were taken on a Nicolet 6700 spectrophotometer by using KBr pellets.

Device Fabrication

Photovoltaic devices were fabricated on 15 × 15 mm^2 patterned indium tin oxide (ITO) coated glass substrates with a layered structure of ITO/PEDOT:PSS(40 nm)/polymer:$PC_{61}BM$ blend (~80 nm)/Ca(10 nm)/Al(100 nm). The ITO coated glass substrates were ultrasonically cleaned sequentially with detergent, water, acetone, and isopropyl alcohol. The substrates were then oxygen plasma treated for 6 min, spin coated with PEDOT:PSS at 4000 rpm, and annealed in an oven for 20 min at 160°C. The polymer (**P1**, **P2**, **P3**) and $PC_{61}BM$ were dissolved in deoxygenated anhydrous *o*-dichlorobenzene (*o*-DCB) in the weight ratios 1.5 : 1, 1 : 1 and 1 : 2 respectively and total concentration of the polymer/$PC_{61}BM$ blending solution was 25 mg mL^{-1}. The solutions were stirred overnight in a nitrogen filled glovebox. An active layer consisting of the blend of polymer and $PC_{61}BM$ was then spin coated on PEDOT:PSS. Subsequently, Ca (10 nm) and Al (100 nm) were thermally

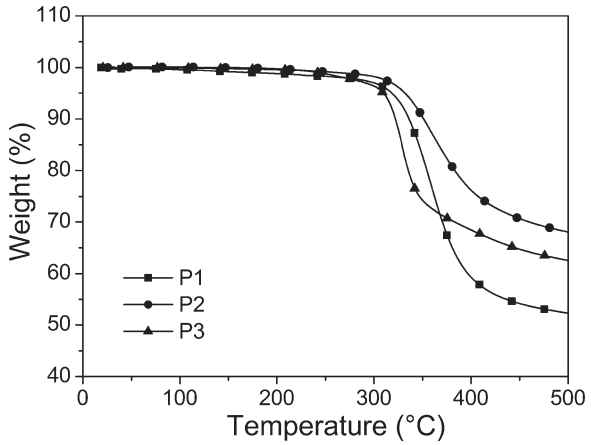

Figure 1. TGA thermograms of **P1–P3** with a heating rate of 10°C min^{-1} under nitrogen atmosphere.

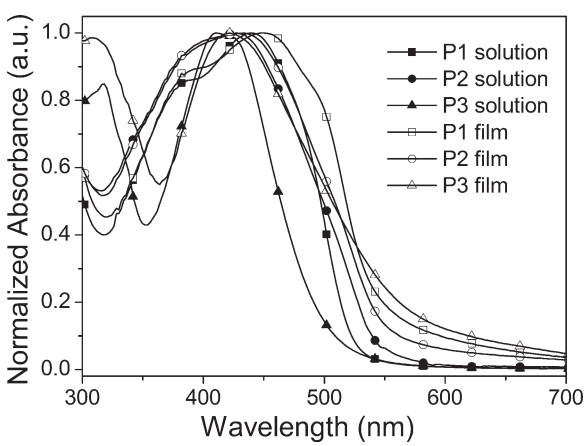

Figure 2. UV–vis absorption spectra of **P1–P3** in chloroform solutions and in thin films.

Table I. Optical and Thermal Properties of **P1–3**

Polymer	Solution[a]		Thin film			Thermal
	λ_{max} (nm)	λ_{onset} (nm)	λ_{max} (nm)	λ_{onset} (nm)	E_g^{opt} (eV)[b]	T_d (°C)
P1	436	521	454	540	2.30	319
P2	427	527	437	528	2.35	332
P3	410	503	424	536	2.31	310

[a] Absorption data was collected in $CHCl_3$ solution.
[b] Data was taken by the absorption edge of the thin film, $E_g^{opt} = 1240/\lambda_{onset}$.

evaporated at a vacuum of $\sim 2 \times 10^{-4}$ Pa on top of active layer as cathode. The cathode area defines active area of the devices, which is 0.1 cm^2. Photovoltaic performance was characterized under illumination with an AM 1.5 G (100 mW cm^{-2}) in an argon atmosphere (<0.1 ppm H_2O and O_2), and current density vs. voltage (*J–V*) curves were recorded by Keithley 2420. External quantum efficiencies (EQE) of solar cells were analyzed by certified Newport incident photon conversion efficiency (IPCE) measurement system.

RESULTS AND DISCUSSION

Synthesis and Characterization

Synthetic routes (Supporting Information Scheme S1) and details for the monomers and polymers are described in Supporting Information. **P1** and **P2** were synthesized by palladium-catalyzed Stille coupling reactions. **P3** was obtained through the palladium-catalyzed Suzuki coupling method. Typical IR spectra for the polymers are shown in Supporting Information Figure S1. All the polymers showed characteristic IR absorption bands of S—C=C stretching (1530 cm^{-1}) and S—C stretching (1448, 1260 cm^{-1}). The typical IR spectra of **P1** showed characteristic band associated with C—O at around 1034 cm^{-1}.[25,26] The structures of polymers were further determined with ^{1}H-NMR spectra, which are consistent with the proposed ones. The peaks due to aromatic protons appear at around δ 8.5–6.5 ppm. The peaks at around δ 3.0 ppm are attributed to the CH_2—S groups and those at around δ 4.4–4.0 ppm are due to the O—CH_2 group (**P1**). The three polymers are soluble in common organic solvents, such as chloroform, chlorobenzene (CB), and *o*-DCB. The molecular weight and polydispersity index (PDI) were determined by GPC with calibration against polystyrene standards. The number average molecular weight of **P1**, **P2**, and **P3** was found to be 50.3, 49.2, and 12.7 kg mol^{-1}, with PDI of 1.8, 1.7, and 2.5, respectively. The obtained high molar masses and narrow PDI of **P1** and **P2** are generally helpful to improve PSC performance by enhancing J_{sc} and FF.[27]

Thermal Properties

Thermal stabilities of the polymers were determined by TGA under nitrogen atmosphere at a heating rate of 10°C min^{-1}. The three polymers show good stability with onset decomposition temperatures corresponding to 5% weight loss at 319°C, 332°C, and 310°C, respectively, as shown in Figure 1. Obviously, the thermal stability of these polymers is adequate for their applications in PSCs and other optoelectronic devices.[28]

Optical and Electrochemical Properties

The optical properties of the three polymers were investigated by UV–vis absorption spectroscopy. The absorption spectra of **P1–P3** in chloroform solutions and thin solid films are shown in Figure 2. In dilute chloroform solutions, the absorption peaks of **P1**, **P2**, and **P3** located at 436 nm, 427 nm, and 410 nm, respectively. In films, the absorption peak of **P1** is located at about 454 nm, **P2** at 437 nm, and **P3** at 424 nm. The detailed data are summarized in Table I. The absorption spectra of **P1**, **P2**, and **P3** in films are broader and red-shifted relative to those in solutions, which is ascribed to the enhanced intermolecular interactions between the polymer main chains[25] and the strong self-assembling propensity of DTF side chains. The optical band gap (E_g^{opt}) of **P1**, **P2**, and **P3** can be estimated at

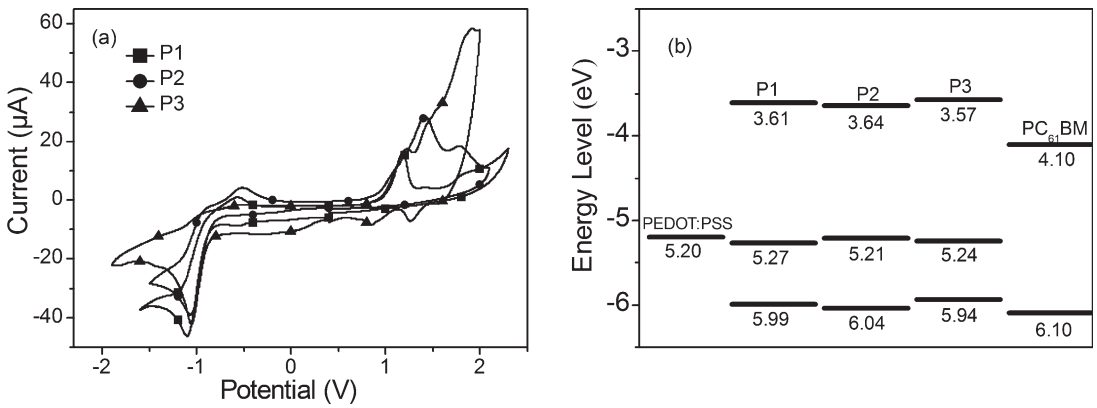

Figure 3. Cyclic voltammograms (a) and HOMO and LUMO energy levels (b) of **P1–P3.**

Table II. Electrochemical Properties of **P1–3**

Polymer	E_{on}^{red} /LUMO (V/eV)	E_{on}^{ox1} /HOMO (V/eV)	E_{on}^{ox2} /HOMO-1 (V/eV)	E_{g1}^{EC} (eV)	E_{g2}^{EC} (eV)
P1	−0.80/−3.61	0.86/−5.27	1.58/−5.99	1.66	2.38
P2	−0.77/−3.64	0.80/−5.21	1.63/−6.04	1.57	2.40
P3	−0.84/−3.57	0.83/−5.24	1.53/−5.94	1.67	2.37

HOMO = $-(E_{on}^{ox} + 4.41)$ eV and LUMO = $-(E_{on}^{red} + 4.41)$ eV, where E_{on}^{red}, E_{on}^{ox} are calculated vs. SCE. E_g^{EC} = LUMO−HOMO.

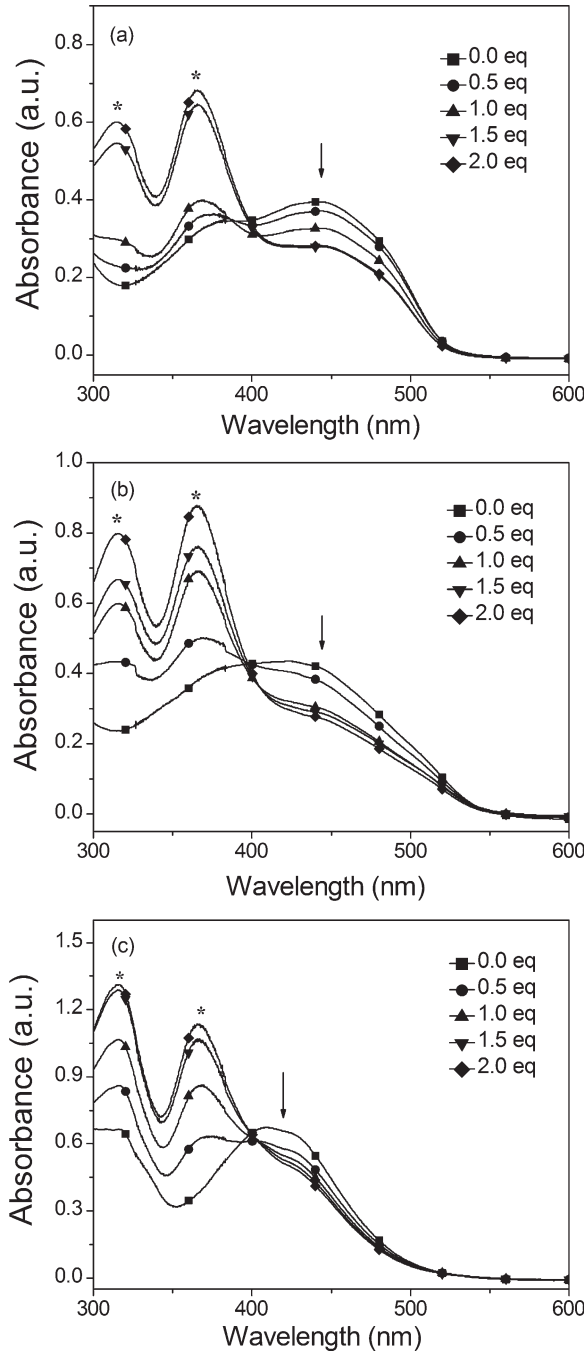

Figure 4. UV–vis absorption spectra of **P1** (a), **P2** (b), and **P3** (c) during chemical oxidation by the successive addition of $FeCl_3$ as an oxidant in $CHCl_3$ at room temperature. Symbol * denotes unreacted $FeCl_3$.

2.30, 2.35, and 2.31 eV, respectively, from their onset absorption in the thin films.

HOMO and LUMO energy levels of the polymers are crucial for the selection of appropriate acceptor materials in PSCs. CV was employed to evaluate the electrochemical properties and electronic energy levels of polymers. Figure 3(a) shows the cyclic voltammograms of the polymers and similar electrochemical characteristics were recorded. The onsets of reduction peak of **P1**, **P2**, and **P3** were observed at −0.80, −0.77, and −0.84 V vs. SCE, corresponding LUMO levels at −3.61, −3.64, and −3.57 eV. The energy differences in the LUMO levels of **P1**/$PC_{61}BM$, **P2**/$PC_{61}BM$, and **P3**/$PC_{61}BM$ were 0.49, 0.46, and 0.53 eV, suggesting that the photo-excited electrons can effectively transfer from the polymers to $PC_{61}BM$.[29–31] As shown in Figure 3(a), the polymers display two oxidation processes. The onsets of the first oxidation of **P1**, **P2**, and **P3** were observed at 0.86, 0.80, and 0.83 V vs. SCE, corresponding HOMO levels at −5.27, −5.21, and −5.24 eV. The band gaps of polymers normally can be deduced by CV from the difference of the onsets of oxidation and reduction processes.[13] As a result, the electrochemical band gap (E_{g1}^{EC}) of 1.66, 1.57, and 1.67 eV for **P1**, **P2**, and **P3** can be obtained, which were much lower than those of E_g^{opt}. Similar phenomenon had been found by Hou et al.,[11] Berridge et al.,[20] and Skabara et al.,[32] when they studied the electrochemical properties of some TTF-containing polymers. Considering the strong electron donating ability of bis(thioether)-substituted dithiol, we assume that the first oxidation process evolves from the bis(thioether)-substituted dithiol, and the electrochemical process is independent of the conjugated main chain, which should not be used in the determination of the band gaps of the polymers.[11,20,32] The onsets of the

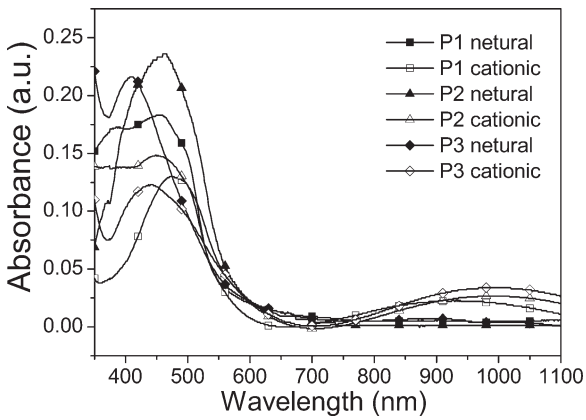

Figure 5. UV–vis absorption spectra of **P1–P3** on ITO glass in the neutral and cationic states.

Table III. PSCs Device Performance with Configuration of ITO/PEDOT : PSS/Polymer : $PC_{61}BM$/Ca/Al

Active layer	Ratio	V_{oc} (V)	J_{sc} (mA cm^{-2})	FF (%)	PCE (%)
P1:$PC_{61}BM$	1.5 : 1	0.85	1.51	30.65	0.39
P2:$PC_{61}BM$	1 : 1	0.80	3.07	42.83	1.05
P3:$PC_{61}BM$	1 : 2	0.61	1.05	24.59	0.16

second oxidation of **P1**, **P2**, and **P3** were observed at 1.58, 1.63, and 1.53 V vs. SCE, and corresponding HOMO-1 levels at −5.99, −6.04, and −5.94 eV. When the onset of the second oxidation peak is used for estimating the electrochemical band gap (E_{g2}^{EC}), then the E_{g2}^{EC}obtained is 2.38, 2.40, and 2.37 eV for **P1**, **P2**, and **P3**, respectively, which are in close agreement with E_g^{opt}. Relevant data are summarized in Table II, and the electronic energy level diagram of the three polymers and $PC_{61}BM$[30] is depicted in Figure 3(b).

Previous works showed that the TTF units could be oxidized to TTF•$^+$, and TTF•$^+$ gave rise to an additional band at 800–1100 nm in the UV–vis spectra.[11,20,32] In order to probe the optical responses of DTF to chemical redox processes, UV–vis spectra analysis on the three polymers after oxidation by $FeCl_3$ in $CHCl_3$ solution was also conducted. As shown in Figure 4(a), upon increasing oxidation, the strong π–π^* transition absorbing band of **P1** at 436 nm decreases gradually and two new bands evolve at 315 and 367 nm, which are assigned to unreacted $FeCl_3$ (Supporting Information Figure S2). One can observe that **P2** and **P3** show similar absorption changes when increasing the oxidant [Figure 4(b,c].

To further investigate their optical responses to electrochemical redox processes, the UV–vis absorption spectra of polymer films were characterized in both neutral and oxidized states. The measurements were performed on the thin films of the three polymers which were spin-coated onto ITO glass. In our experiments, each UV–vis spectral scan was performed after the electrolysis of an analyte at a controlled voltage [1.1, 1.4, and 1.2 V for **P1**, **P2**, and **P3** respectively, which were the first oxidation peak potential obtained from Figure 3(a)] for at least 180 s to ensure the electric current attained a constant value.[33] As such, the systems examined by UV–vis spectroscopy can be deemed as having arrived at equilibrium. As shown in Figure 5, the thin film of **P1** (neutral state) showed a strongly absorbing π–π^* transition band at 454 nm. After being subjected to electrolysis at 1.1 V for 180 s, the thin film color of **P1** was observed to change from yellow to brown. The UV–vis spectrum of oxidized **P1** shows a new broad low-energy band covering the spectral range of 750–1100 nm. Meanwhile the absorption peak at 454 nm is greatly attenuated which agrees with the UV–vis spectra of **P1** when it was oxidized by $FeCl_3$ in solution. **P2** and **P3** show similar absorption changes as increasing oxidation. Previous reports involving absorption studies on TTF-containing polymers[11,20,32] have also shown that upon oxidation, the resulting TTF•$^+$ species give rise to an additional band at 800–1100 nm, which can be assigned to a unique feature of the cation radical species. Thus, we assume that the new broad band should be assigned to DTF oxidation species (DTF•$^+$). The results are consistent with the cyclic voltammograms.

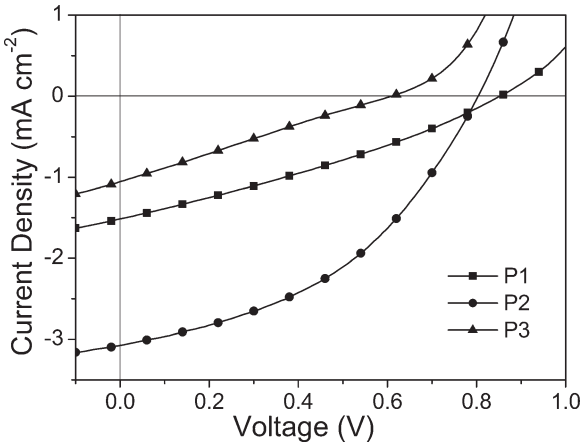

Figure 6. *J–V* curves of polymer/$PC_{61}BM$-based regular single solar cells under AM 1.5 G illumination, 100 mW cm^{-2}.

Photovoltaic Performance

The bulk heterojunction PSCs were fabricated to investigate the photovoltaic effects of the polymers with a device structure of ITO/PEDOT:PSS/polymer:$PC_{61}BM$ /Ca/Al, and measured under a simulated AM 1.5 G illumination of 100 mW cm^{-2}. The optimized blend weight ratios of **P1** (**P2**, **P3**) and $PC_{61}BM$ were 1.5 : 1 (1 : 1, 1 : 2). The active layers of these devices were spin-coated from the *o*-DCB solutions of corresponding blends. The V_{oc}, J_{sc}, FF, and PCE of the devices are listed in Table III and their *J–V* curves are shown in Figure 6. Due to the lower HOMO level of the polymers, our systems show higher V_{oc} values when compared with TTF-fused polymers reported in the literature (V_{oc} = 0.42–0.52 V).[11,20] **P2** exhibited the best PCE of 1.05% with a V_{oc} of 0.80 V, a J_{sc} of 3.07 mA cm^{-2}, and an FF of 42.8%. As depicted by CVs and UV–vis absorption spectra, DTF can be oxidized to DTF•$^+$, the resulting formation of DTF•$^+$ may lead to increase in rigidity of the conjugated polymer side chain and conformational changes in the polymer due to the on-site Coulombic repulsion,[33–36] which may lead to decreases in exciton propagation lengths. This may be the potential reason for the small J_{sc} and low PCE. Although the PCE and FF are relatively low, to our best knowledge, it is the highest one among the reported TTF-fused ensembles[11,20] and DTF-fused ensembles.[24] EQE curves of the devices based on these polymers prepared through the optimal fabrication process are shown in Supporting Information Figure S3. Due to the wide optical band gaps of the polymers, the three devices show a narrow response range, only covering from 320 to 550 nm.

CONCLUSIONS

Three DTF-fused polymers were synthesized and characterized. These polymers have good thermal stability with decomposition temperatures higher than 300°C. The electrochemical characteristics

and UV–vis absorption spectroscopy indicated that the DTF moiety could be oxidized to DTF•$^+$, and the process was independent of the conjugated main chain of the polymer. Upon increasing oxidation, the strong π–π^* transition absorbing band of the three polymers decreases gradually, and the resulting DTF•$^+$ species give rise to an additional band at 750–1100 nm, which can be assigned to a distinguishing feature of the cation radical species. The photovoltaic effect of the polymers was investigated, and **P2** exhibited the best PCE of 1.05%, higher than all the reported TTF-fused and DTF-fused ensembles. More efforts to increase the optical absorbance and thus improve the photovoltaic performance of DTF containing polymers are currently on going in our group.

ACKNOWLEDGMENTS

This work was supported by National Natural Science Foundation of China (21202181, 21204097, 51173199, 51303197, 61107090), Ministry of Science and Technology of China (2010DFA52310), and Department of Science and Technology of Shandong Province (ZR2012BQ021).

REFERENCES

1. Zhang, M.; Gu, Y.; Guo, X.; Liu, F.; Zhang, S.; Huo, L.; Russell, T. P.; Hou, J. *Adv. Mater.* **2013**, *25*, 4944.
2. Chen, H.-C.; Chen, Y.-H.; Liu, C.-C.; Chien, Y.-C.; Chou, S.-W.; Chou, P.-T. *Chem. Mater.* **2012**, *4*, 4766.
3. Wen, S.; Bao, X.; Shen, W.; Gu, C.; Du, Z.; Han, L.; Zhu, D.; Yang, R. *J. Polym. Sci. Part A: Polym. Chem.* **2014**, *52*, 208.
4. Wang, Y.; Liu, Y.; Chen, S.; Peng, R.; Ge, Z. *Chem. Mater.* **2013**, *25*, 3196.
5. Cabanetos, C.; El Labban, A.; Bartelt, J. A.; Douglas, J. D.; Mateker, W. R.; Frechet, J. M.; McGehee, M. D.; Beaujuge, P. M. *J. Am. Chem. Soc.* **2013**, *135*, 4656.
6. Yuan, J.; Zhai, Z.; Dong, H.; Li, J.; Jiang, Z.; Li, Y.; Ma, W. *Adv. Funct. Mater.* **2013**, *23*, 885.
7. Wang, X.; Jiang, P.; Chen, Y.; Luo, H.; Zhang, Z.; Wang, H.; Li, X.; Yu, G.; Li, Y. *Macromolecules* **2013**, *46*, 4805.
8. Giovanella, U.; Botta, C.; Galeotti, F.; Vercelli, B.; Battiato, S.; Pasini, M. *J. Mater. Chem. C* **2013**, *1*, 5322.
9. Poduval, M. K.; Burrezo, P. M.; Casado, J.; López Navarrete, J. T.; Ortiz, R. P.; Kim, T.-H. *Macromolecules* **2013**, *46*, 9220.
10. Ouchi, M.; Badi, N.; Lutz, J. F.; Sawamoto, M. *Nat. Chem.* **2011**, *3*, 917.
11. Hou, Y.; Chen, Y.; Liu, Q.; Yang, M.; Wan, X.; Yin, S.; Yu, A. *Macromolecules* **2008**, *41*, 3114.
12. Zhou, H.; Yang, L.; Stuart, A. C.; Price, S. C.; Liu, S.; You, W. *Angew. Chem. Int. Edit.* **2011**, *50*, 2995.
13. You, J.; Dou, L.; Yoshimura, K.; Kato, T.; Ohya, K.; Moriarty, T.; Emery, K.; Chen, C. C.; Gao, J.; Li, G.; Yang, Y. *Nat. Commun.* **2013**, *4*, 1446.
14. Cheng, Y.-J.; Yang, S.-H.; Hsu, C.-S. *Chem. Rev.* **2009**, *109*, 5868.
15. Bryce, M. R. *J. Mater. Chem.* **2000**, *10*, 589.
16. Canevet, D.; Salle, M.; Zhang, G.; Zhang, D.; Zhu, D. *Chem. Commun (Camb)* **2009**, 2245.
17. Gao, F.; Cui, L.; Liu, W.; Hu, L.; Zhong, Y. W.; Li, Y. Z.; Zuo, J. L. *Inorg. Chem.* **2013**, *52*, 11164.
18. Lemouchi, C.; Meziere, C.; Zorina, L.; Simonov, S.; Rodriguez-Fortea, A.; Canadell, E.; Wzietek, P.; Auban-Senzier, P.; Pasquier, C.; Giamarchi, T.; Garcia-Garibay, M. A.; Batail, P. *J. Am. Chem. Soc.* **2012**, *134*, 7880.
19. de Caro, D.; Valade, L.; Faulmann, C.; Jacob, K.; Van Dorsselaer, D.; Chtioui, I.; Salmon, L.; Sabbar, A.; El Hajjaji, S.; Pérez, E.; Franceschi, S.; Fraxedas, J. *New J. Chem.* **2013**, *37*, 3331.
20. Berridge, R.; Skabara, P. J.; Pozo-Gonzalo, C.; Kanibolotsky, A.; Lohr, J.; McDouall, J. J. W. *J. Phys. Chem. B* **2006**, *110*, 3140.
21. Bond, A. M.; Bano, K.; Adeel, S.; Martin, L. L.; Zhang, J. *ChemElectroChem* **2014**, *1*, 99.
22. Pop, F.; Amacher, A.; Avarvari, N.; Ding, J.; Daku, L. M. L.; Hauser, A.; Koch, M.; Hauser, J.; Liu, S.-X.; Decurtins, S. *Chem.—Eur. J.* **2013**, *19*, 2504.
23. Hou, Y.; Long, G.; Sui, D.; Cai, Y.; Wan, X.; Yu, A.; Chen, Y. *Chem. Commun. (Camb)* **2011**, *47*, 10401.
24. Chen, Y.-C.; Hsu, C.-Y.; Lin, J. T. *J. Polym. Sci. Part A: Polym. Chem.* **2012**, *50*, 2121.
25. Sun, X.; Chen, W.; Du, Z.; Bao, X.; Song, G.; Guo, K.; Wang, N.; Yang, R. *Polym. Chem.* **2013**, *4*, 1317.
26. Liu, Q.; Du, Z.; Chen, W.; Sun, L.; Chen, Y.; Sun, M.; Yang, R. *Synth. Met.* **2013**, *178*, 38.
27. Dou, L.; You, J.; Yang, J.; Chen, C. C.; He, Y.; Murase, S.; Moriarty, T.; Emery, K.; Li, G.; Yang, Y. *Nat. Photon.* **2012**, *6*, 180.
28. Wang, X.; Sun, Y.; Chen, S.; Guo, X.; Zhang, M.; Li, X.; Li, Y.; Wang, H. *Macromolecules* **2012**, *45*, 1208.
29. Dou, L.; Chen, C.-C.; Yoshimura, K.; Ohya, K.; Chang, W.-H.; Gao, J.; Liu, Y.; Richard, E.; Yang, Y. *Macromolecules* **2013**, *46*, 3384.
30. Baek, M.-J.; Lee, S.-H.; Zong, K.; Lee, Y.-S. *Synth. Met.* **2010**, *160*, 1197.
31. Koster, L. J. A.; Mihailetchi, V. D.; Blom, P. W. M. *Appl. Phys. Lett.* **2006**, *88*, 093511.
32. Skabara, P. J.; Berridge, R.; McInnes, E. J. L.; West, D. P.; Coles, S. J.; Hursthouse, M. B.; Müllen, K. *J. Mater. Chem.* **2004**, *14*, 1964.
33. Chen, G.; Mahmud, I.; Dawe, L. N.; Daniels, L. M.; Zhao, Y. *J. Org. Chem.* **2011**, *76*, 2701.
34. Yamashita, Y.; Tomura, M.; Imaeda, K. *Tetrahedron Lett.* **2001**, *42*, 4191.
35. Yamashita, Y.; Tomura, M.; Tanaka, S.; Imaeda, K. *Synth. Met.* **1999**, *102*, 1730.
36. Yamashita, Y.; Tomura, M.; Zaman, M. B. *Chem. Commun.* **1998**, 1657.